Volume 52 | Number 48 | 18 June 2016 | Pages 7519–7622

ChemComm

Chemical Communications

www.rsc.org/chemcomm

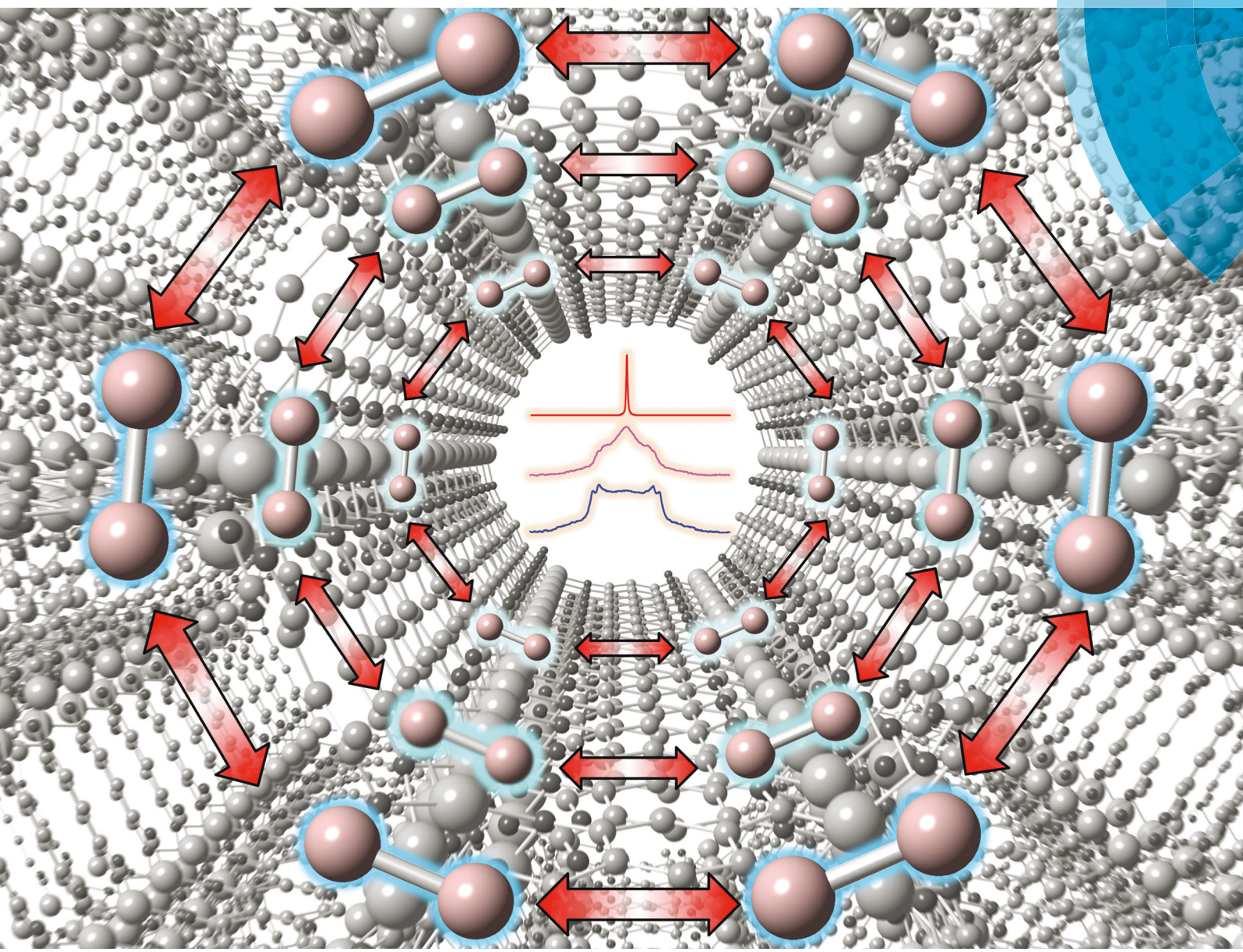

ISSN 1359-7345

ROYAL SOCIETY OF CHEMISTRY

COMMUNICATION

Yining Huang *et al.*

Grasping hydrogen adsorption and dynamics in metal–organic frameworks using ^{2}H solid-state NMR

175 YEARS

ChemComm

COMMUNICATION

View Article Online
View Journal | View Issue

Open Access Article. Published on 04 May 2016. Downloaded on 5/9/2026 8:09:54 AM.
This article is licensed under a Creative Commons Attribution-NonCommercial 3.0 Unported Licence.

Cite this: *Chem. Commun.*, 2016, 52, 7541

Received 16th April 2016,
Accepted 4th May 2016

DOI: 10.1039/c6cc03205b

www.rsc.org/chemcomm

Grasping hydrogen adsorption and dynamics in metal–organic frameworks using ^{2}H solid-state NMR†

Bryan E. G. Lucier,‡ Yue Zhang,‡ Kelly J. Lee, Yuanjun Lu and Yining Huang*

Record greenhouse gas emissions have spurred the search for clean energy sources such as hydrogen (H_2) fuel cells. Metal–organic frameworks (MOFs) are promising H_2 adsorption and storage media, but knowledge of H_2 dynamics and adsorption strengths in these materials is lacking. Variable-temperature (VT) ^{2}H solid-state NMR (SSNMR) experiments targeting $^2H_2$ gas (*i.e.*, D_2) shed light on D_2 adsorption and dynamics within six representative MOFs: UiO-66, M-MOF-74 (M = Zn, Mg, Ni), and α-$M_3(COOH)_6$ (M = Mg, Zn). D_2 binding is relatively strong in Mg-MOF-74, Ni-MOF-74, α-$Mg_3(COOH)_6$, and α-$Zn_3(COOH)_6$, giving rise to broad ^{2}H SSNMR powder patterns. In contrast, D_2 adsorption is weaker in UiO-66 and Zn-MOF-74, as evidenced by the narrow ^{2}H resonances that correspond to rapid reorientation of the D_2 molecules. Employing ^{2}H SSNMR experiments in this fashion holds great promise for the correlation of MOF structural features and functional groups/metal centers to H_2 dynamics and host–guest interactions.

Carbon dioxide (CO_2) is associated with the greenhouse effect and global warming. H_2 fuel cells and other "greener" solutions are the future energy sources for automobiles, however, many proposals for H_2 storage involve tanks for compressed H_2,[1] which is flammable and explosive. Safer alternatives for H_2 storage, such as crystalline materials,[1,2] are desired. Metal–organic frameworks (MOFs) are ordered three-dimensional structures consisting of metal centers or metal–inorganic units joined by organic linkers. By varying the MOF topology, metal center, and linkers,[3] tailored large surface areas and guest binding strengths are possible. Several MOFs have shown H_2 adsorption and storage capabilities,[4] including UiO-66,[5,6] MOF-74,[7] α-$Mg_3(COOH)_6$,[8] and α-$Zn_3(COOH)_6$.[9]

X-ray diffraction is widely used to investigate gas adsorption in MOFs but cannot reliably locate H_2. Neutron diffraction can find H_2 but little motional details can be obtained. Adsorption isotherms provide H_2 capacity yet yield little positional or dynamic data. IR spectroscopy may indicate H_2 adsorption and binding sites, but H_2 motion remains unknown. Computational methods can estimate H_2 location and dynamics, yet demand experimental verification. In order to (i) move MOFs toward practical incorporation as H_2 storage media, and (ii) enhance H_2 capacity in future MOFs, knowledge of the dynamic behavior of H_2 in today's MOFs is critical. SSNMR is a sensitive probe of the local nuclear electronic and magnetic environment, and provides rich information on MOFs from the perspective of the metals,[10] organic linkers,[11] guest molecules,[12] and dynamic components.[13,14] NMR interactions are generally anisotropic (directionally-dependent) with respect to the magnetic field and are influenced by dynamics in a predictable manner; rich motional information can be extracted from spectral simulations.[15]

When dynamics are of interest in NMR, the ^{2}H isotope is preferred over ^{1}H. ^{2}H has a spin of 1 and is subject to the anisotropic quadrupolar interaction (QI) between the nuclear quadrupole moment and surrounding electric field gradients (EFGs). Any motion that reorients the ^{2}H EFG tensor influences the QI; since the ^{2}H SSNMR spectrum is dominated by the QI, ^{2}H SSNMR is a powerful probe of guest dynamics. ^{1}H is a spin-1/2 nucleus that suffers from very strong ^{1}H–^{1}H homonuclear dipolar coupling in solids, resulting in broad ^{1}H SSNMR spectra that rarely yield useful information. ^{2}H SSNMR has proven to be an effective tool for studying the binding in metal–dihydrogen complexes,[16–18] and has been successfully used to probe D_2 mobility within a Ru-modified MOF.[19] Wright *et al.* have shown that ^{2}H SSNMR provides rich information on the dynamics of deuterated linkers and guests in MOFs and microporous materials.[20–24] Herein, we use VT ^{2}H SSNMR to probe H_2 adsorption in a series of different MOFs, studying the significant differences in D_2 adsorption behavior and dynamics within UiO-66, M-MOF-74 (M = Zn, Mg, Ni), and α-$M_3(COOH)_6$ (M = Mg, Zn).

UiO-66[6] is a three-dimensional MOF composed of $Zr_6O_4(OH)_4$ units and 1,4-benzenedicarboxylate (BDC) linkers, with large octahedral and tetrahedral cages with pore sizes *ca.* 11 Å and 8 Å,

Department of Chemistry, The University of Western Ontario, 1151 Richmond Street, London, Ontario, N6A 5B7, Canada. E-mail: yhuang@uwo.ca

† Electronic supplementary information (ESI) available: Full details of MOF synthesis, D_2 loading, and SSNMR experiments. Illustrations of the MOFs, H_2/D_2 adsorption sites in MOF-74, additional ^{2}H SSNMR spectra and simulations, tables, and powder XRD patterns are also included. See DOI: 10.1039/c6cc03205b

‡ These authors contributed equally to this work.

Open Access Article. Published on 04 May 2016. Downloaded on 5/9/2026 8:09:54 AM.
This article is licensed under a Creative Commons Attribution-NonCommercial 3.0 Unported Licence.

respectively (Fig. S1, ESI†). VT ^{2}H SSNMR spectra of D_2 in UiO-66 (Fig. S2, ESI†) feature a narrow resonance from 293 K to 133 K with a full width at half height (FWHH) of 45 Hz throughout. Although D_2 is adsorbed in UiO-66, the large pores permit rapid diffusion of D_2 guests through the MOF void space,[5] eliminating the spectral broadening effects of the QI and giving rise to a sharp, motionally-averaged ^{2}H resonance. The narrow lineshape indicates that any localized MOF–D_2 interactions are relatively weak and easily overcome by diffusion. The tetrahedral and octahedral pore geometries may also contribute to the observed narrow resonance.

M-MOF-74 (M = metal) is composed of metal centers connected by 2,5-dioxido-1,4-benzenedicarboxylate (dobdc) linkers that form honeycomb-shaped channels *ca.* 11 Å wide with metal centers at each vertex (Fig. S3, ESI†). Each metal center is connected to five oxygen atoms from four linkers in the as-made MOF, along with a sixth oxygen from a water molecule that can be removed *via* activation. The resulting coordinatively-unsaturated open metal site (OMS) strongly encourages adsorption of H_2.[7,25] The nature of the metal center influences H_2 binding affinity, which increases in the order Zn < Mg < Ni.[7] The ^{2}H SSNMR spectrum of D_2 in Zn-MOF-74 features a narrow resonance of 80 Hz FWHH at 293 K (Fig. 1(a)), implying that D_2 undergoes rapid isotropic reorientation in the MOF. The FWHH increases to 120 Hz at 213 K and 1920 Hz at 133 K. At lower temperatures, D_2 motion is reduced, leading to a large increase in FWHH. The ^{2}H resonance widths in Zn-MOF-74 are much larger than in UiO-66 at all temperatures, indicating that D_2 is considerably less mobile in Zn-MOF-74 due to metal–H_2 interactions; however, the lack of spectral features at 133 K confirms that D_2 dynamics remain rapid, and efficient H_2 diffusion pathways in the MOF-74 family are known to exist.[26]

Mg-MOF-74 has a higher affinity for H_2/D_2 and yields the VT SSNMR spectra in Fig. 1(b). The narrow resonance at 293 K corresponds to highly mobile D_2 gas, while emerging broad spectral features at 173 K indicate the onset of significant D_2 adsorption.

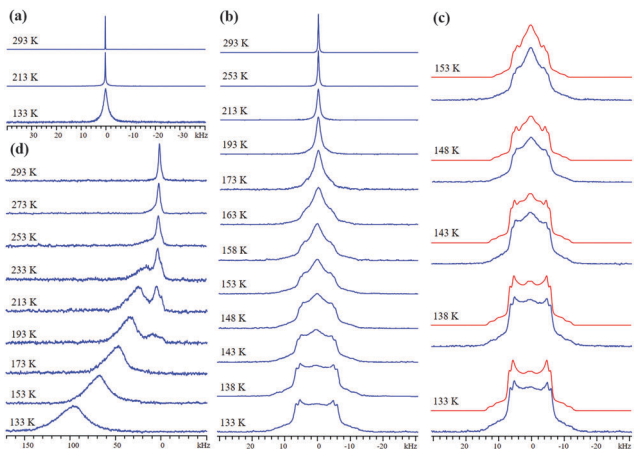

Fig. 1 The experimental static VT ^{2}H SSNMR spectra of adsorbed D_2 within (a) Zn-MOF-74, (b and c) Mg-MOF-74, and (d) Ni-MOF-74 are depicted. Experimental (blue) and simulated (red) ^{2}H SSNMR spectra in Mg-MOF-74 at low temperatures are shown in (c). The sharp resonance at *ca.* 0 kHz in all spectra at high temperatures corresponds to mobile or very weakly adsorbed D_2; this resonance is broadened in (d) due to the influence of the paramagnetic Ni metal center.

At 153 K, adsorbed D_2 gives rise to two broad ^{2}H powder patterns along with a narrow central resonance from free D_2 in the center of the pores. The wide ^{2}H lineshapes at 133 K are intense, well-defined, and associated with most of the D_2 in Mg-MOF-74 (Fig. 1(c)). By comparing the ^{2}H quadrupolar coupling constant (C_Q) of gaseous D_2 (225 kHz[27]) to the apparent C_Qs of D_2 in Mg-MOF-74 (Table S1, ESI†), D_2 dynamic information can be extracted.[18] Observed $C_Q(^2H)$ values in Mg-MOF-74 are far less than 225 kHz, and are also smaller than the $C_Q(^2H)$ range of *ca.* 30–120 kHz associated with η^2 bonding between a metal and D_2 in metal–dihydrogen complexes,[18,28–30] implying that fast D_2 motion exists here and that the metal–D_2 interactions in Mg-MOF-74 are weaker than the bonding in metal–dihydrogen complexes. It should be noted that at the experimental temperatures and magnitudes of quadrupolar coupling in this study, any spectral effects arising from D_2 rotational tunneling are expected to be negligible.[31,32]

The same two powder patterns and NMR parameters persist, along with the sharp component, when the loading level is halved to 0.1 D_2/Mg (Fig. S4 and S5, Table S2, ESI†). The two broad ^{2}H powder patterns of D_2 in Mg-MOF-74 reveal that there are two similar, but nonequivalent D_2 molecules (D_2(1) and D_2(2)) adsorbed on two different OMSs, as indicated by their QI parameters and D_2 motions (see Appendix A in the ESI†), while the narrow third resonance indicates that highly mobile D_2 is also present. Previous studies have suggested that there may be two very similar H_2 adsorption sites of nearly identical adsorption enthalpy localized on the OMS near our experimental loading levels with slightly different interaction geometries.[33,34] There are 6 OMSs located near the same cross-sectional plane per channel (Fig. 2(b)). At a low loading level of 0.1 D_2/metal, on average, there is less than one D_2 guest per channel cross-section. Thus, it is reasonable to assume that no two D_2 molecules are adsorbed simultaneously on the same OMS at any given time. It is likely that each channel cross-section contains only 1 D_2 molecule that is in rapid exchange among the 6 sites (*vide infra*). Based on the intensity ratios in Table S1 (ESI†), *ca.* 59% of the channel cross-sections

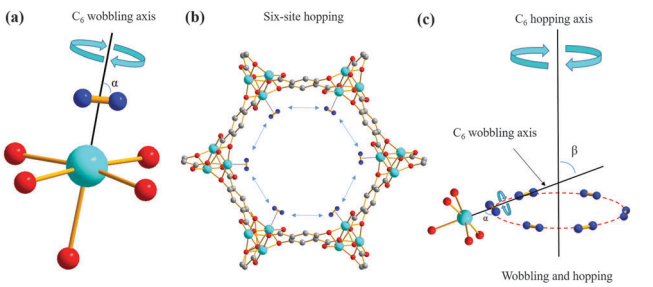

Fig. 2 The localized C_6 rotation, or wobbling, of D_2 molecules adsorbed on the OMS is shown in (a). The black line represents the metal–D_2 vector; the cone of D_2 wobbling movement traces out an angle α about the wobbling axis. A schematic of D_2 hopping in MOF-74 is shown in (b). The combination of wobbling (C_6 rotation, α) and six-site hopping (C_6 rotation, β) of D_2 molecules in MOF-74 is shown in (c), where the wobbling axis makes an angle β with respect to the hopping axis. The colors red, grey, blue and cyan correspond to oxygen, carbon, deuterium and the metal center, respectively. Our data indicate that there are two very similar D_2 adsorption sites on the OMS, giving rise to two separate ^{2}H SSNMR powder patterns.

 This journal is © The Royal Society of Chemistry 2016

Open Access Article. Published on 04 May 2016. Downloaded on 5/9/2026 8:09:54 AM.
This article is licensed under a Creative Commons Attribution-NonCommercial 3.0 Unported Licence.

are populated by $D_2(1)$ and 41% of the channel cross-sections are occupied by $D_2(2)$.

Using the known ^2H QI parameters of D_2 gas ($C_Q(^2H)$ = 225 kHz, $\eta_Q = 0$),[27] simulations[15] of motionally-averaged ^2H spectra (Fig. S6, ESI†) reveal that common D_2 dynamics exist at the two similar adsorption sites on the OMS in Mg-MOF-74 (Fig. 2 and Table S3, ESI†). D_2 undergoes a local rotation or "wobbling" modeled by a sixfold rotation about the minimum energy configuration with respect to the OMS (Fig. 2(a)), as well as a non-localized six-site hopping along the pore edge (Fig. 2(b)). The combined motional model is shown in Fig. 2(c). The wobbling describes a rotation of the D–D bond about the axis passing through the OMS (Fig. 2(a)), as defined by angle α. It is likely that the wobbling rotation represents a model for some kind of rotational diffusion on the OMS. The hopping occurs between six nearly coplanar OMSs, where three reside in one plane, and the other three OMSs are in a very proximate plane slightly offset along the longitudinal direction of the channel. It should be noted that since the wobbling and hopping motional rates are in the fast exchange limit, there are an infinite number of C_n ($n \geq 3$) jumping motions that could lead to the observed powder patterns. The dynamic behavior of D_2 at both adsorption sites is strikingly similar, supporting the notion of two H_2 adsorption sites of nearly identical interaction geometry and enthalpy on the OMS: each has D_2 wobbling angles increasing from *ca.* 74° at 293 K to 82° at 133 K, along with constant hopping angles of *ca.* 60° (Table S3, ESI†). The larger wobbling angle at low temperatures enhances the interaction of D_2 with the Mg site. It should also be noted that simulation of fast-exchange SSNMR spectra can sometimes lead to more than one motional model. However, we were unable to simulate the split "horns" or characteristic "shoulders" of the low-temperature spectra using a single adsorption site with any type of possible motions (Appendix A). These results also suggest that there does not seem to be significant exchange of D_2 between the two adsorption sites; increasing the possibility that the sites are somehow segregated or correspond to slightly different types of OMSs in separate MOF channels. The calculated H_2 position in Co-MOF-74[35] strongly agrees with the orientations in our motional model, while the types of D_2 dynamics resemble those of CO_2 and CO in MOF-74.[36–38] To confirm at low temperatures that the D_2 motional rate remains in the fast (*i.e.*, $\geq 10^7$ Hz) and not in the intermediate regime, quadrupolar echo experiments with different inter-pulse delays were performed, resulting in unchanged spectra (Fig. S7 and S8, Table S4, ESI†).

Ni-MOF-74 has a stronger H_2/D_2 binding affinity.[7] Unlike diamagnetic Zn^{2+} and Mg^{2+}, Ni^{2+} is paramagnetic in this MOF. The ^2H magnetic dipole couples with those of proximate unpaired electrons, resulting in spectral broadening and unusual chemical shifts when D_2 is near Ni^{2+}. VT ^2H SSNMR spectra of D_2 in Ni-MOF-74 (Fig. 2(d)) at room temperature reveal that D_2 is mobile and/or rapidly exchanges with adsorbed D_2. The broad 1.2 kHz FWHH confirms the proximity of D_2 to Ni^{2+}. At 273 K, a second, broader resonance emerges at 140 ppm, corresponding to D_2 adsorbed on the OMS. At 213 K, the broad resonance is at 375 ppm and is the dominant feature. The broad resonance increases in frequency, width, and relative intensity as temperature is reduced; the narrower resonance at lower frequency vanishes at 173 K, implying that most D_2 is adsorbed. At 133 K a broad, featureless ^2H resonance of FWHH 30 kHz centered at about 1550 ppm is evident, confirming that a majority of D_2 is adsorbed onto the OMS. The featureless nature of these resonances prohibits detailed analysis.[39]

α-$Mg_3(COOH)_6$ and α-$Zn_3(COOH)_6$ are porous MOFs[8,9,40] with one-dimensional zig-zag channels of small *ca.* 4–5 Å diameter (Fig. S9, ESI†). The ^2H spectrum of D_2 in α-$Mg_3(COOH)_6$ at 293 K features a narrow resonance of 375 Hz FWHH (Fig. S10(a), ESI†) arising from mobile D_2, flanked by a less intense powder pattern 40 kHz broad at 193 K from adsorbed D_2, in agreement with adsorption isotherms.[8,40] At 133 K the broad powder patterns are of higher S/N, reflecting increased D_2 adsorption in α-$Mg_3(COOH)_6$, and are convoluted with a broad distribution of intensity possibly from disordered D_2; other small guests such as ethanol and methanol are also disordered in this MOF.[40] The ^2H SSNMR spectra of D_2 in α-$Zn_3(COOH)_6$ are of similar lineshape and breadth (Fig. S10(b), ESI†), implying that both MOFs have similar H_2 adsorption strengths. The intense narrow resonance persists at lower temperatures in α-$Zn_3(COOH)_6$, indicating that there is more mobile H_2 in α-$Zn_3(COOH)_6$ at all temperatures. The complicated powder patterns are clear evidence of multiple D_2 adsorption sites within both α-$Mg_3(COOH)_6$ and α-$Zn_3(COOH)_6$. At 0.1 D_2/metal loading, in addition to free gas, ^2H spectra may be simulated using three and two adsorption sites in α-$Mg_3(COOH)_6$ and α-$Zn_3(COOH)_6$, respectively. In strong agreement with our experimental observations is a very recent study that has located three main H_2 adsorption sites in α-$Mg_3(COOH)_6$.[41]

The ^2H spectrum of α-$Zn_3(COOH)_6$ is less ambiguous, of higher resolution, and is more straightforward to simulate (Fig. S10(c), Tables S3 and S5, ESI†). The well-defined ^2H SSNMR spectra of D_2 in α-$Zn_3(COOH)_6$ yield relatively high η_Q values along with C_Q values *ca.* 5–10 kHz greater than those of D_2 in Mg-MOF-74 at all equivalent temperatures, reflecting reduced D_2 mobility and perhaps a stronger D_2-MOF interaction in α-$Zn_3(COOH)_6$. In contrast, the very complicated ^2H spectra of α-$Mg_3(COOH)_6$ permit only a preliminary motional simulation at this time (Fig. S11, ESI†). A combined wobbling and hopping of D_2 occurs at all adsorption sites in both systems. D_2 hops between two adsorption sites in α-$Zn_3(COOH)_6$, reminiscent of the twofold hopping by CO_2 guests in the α-$M_3(COOH)_6$ MOF.[42] It is notable that the changes in D_2 motional angles within Zn are not very pronounced across the experimental temperature range (Table S3, ESI†). At this point, the nature of the adsorption sites is unclear from SSNMR experiments. We are currently performing more detailed studies in order to extract detailed D_2 motional and adsorption information from both α-$M_3(COOH)_6$ MOFs.

^2H SSNMR spectroscopy has revealed unique insights into H_2 dynamics and adsorption locations within these six MOFs; this information is unavailable or very difficult to obtain using traditional MOF characterization methods such as adsorption isotherms and X-ray diffraction. Complementary methods such as neutron diffraction, inelastic neutron scattering, and VT infrared spectroscopy are necessary to locate adsorption locations, but yield limited motional data. Variation of the MOF topology,

Open Access Article. Published on 04 May 2016. Downloaded on 5/9/2026 8:09:54 AM.
This article is licensed under a Creative Commons Attribution-NonCommercial 3.0 Unported Licence.

metal center, and linker gives rise to very different D_2 dynamic behaviors and adsorption strengths. Further studies employing lower temperatures (*i.e.*, <100 K) are necessary to reduce H_2 mobility and obtain richer dynamic knowledge in these systems, however, these experiments are not yet possible with the equipment available to us. We have used relatively low levels of D_2 loading to simplify these systems for spectral simulations; the next step is to explore higher D_2 loading levels in order to understand the implications for H_2 motion in a practical hydrogen storage setting. The comprehensive molecular-level knowledge of H_2 dynamics and adsorption in MOFs available from ^{2}H SSNMR spectroscopy will undoubtedly assist in establishing clear links between H_2 dynamics and high-capacity H_2 storage in porous materials, with clear applications in green energy solutions.

Y. H. thanks the Natural Science and Engineering Research Council (NSERC) of Canada for a Discovery grant and a Discovery Accelerator Supplements Award. We also thank an anonymous Reviewer for the helpful input and suggestions.

References

1 D. J. Durbin and C. Malardier-Jugroot, *Int. J. Hydrogen Energy*, 2013, **38**, 14595–14617.
2 J. Yang, A. Sudik, C. Wolverton and D. J. Siegel, *Chem. Soc. Rev.*, 2010, **39**, 656–675.
3 M. D. Allendorf and V. Stavila, *CrystEngComm*, 2015, **17**, 229–246.
4 M. P. Suh, H. J. Park, T. K. Prasad and D.-W. Lim, *Chem. Rev.*, 2012, **112**, 782–835.
5 S. Chavan, J. G. Vitillo, D. Gianolio, O. Zavorotynska, B. Civalleri, S. Jakobsen, M. H. Nilsen, L. Valenzano, C. Lamberti, K. P. Lillerud and S. Bordiga, *Phys. Chem. Chem. Phys.*, 2012, **14**, 1614–1626.
6 J. H. Cavka, S. Jakobsen, U. Olsbye, N. Guillou, C. Lamberti, S. Bordiga and K. P. Lillerud, *J. Am. Chem. Soc.*, 2008, **130**, 13850–13851.
7 W. Zhou, H. Wu and T. Yildirim, *J. Am. Chem. Soc.*, 2008, **130**, 15268–15269.
8 B. Schmitz, I. Krkljus, E. Leung, H. W. Höffken, U. Müller and M. Hirscher, *ChemSusChem*, 2010, **3**, 758–761.
9 Z. Wang, Y. Zhang, M. Kurmoo, T. Liu, S. Vilminot, B. Zhao and S. Gao, *Aust. J. Chem.*, 2006, **59**, 617–628.
10 P. He, B. E. G. Lucier, V. V. Terskikh, Q. Shi, J. X. Dong, Y. Y. Chu, A. M. Zheng, A. Sutrisno and Y. N. Huang, *J. Phys. Chem. C*, 2014, **118**, 23728–23744.
11 D. I. Kolokolov, A. G. Stepanov, V. Guillerm, C. Serre, B. Frick and H. Jobic, *J. Phys. Chem. C*, 2012, **116**, 12131–12136.
12 D. I. Kolokolov, H. Jobic, S. Rives, P. G. Yot, J. Ollivier, P. Trens, A. G. Stepanov and G. Maurin, *J. Phys. Chem. C*, 2015, **119**, 8217–8225.
13 K. Zhu, C. A. O'Keefe, V. N. Vukotic, R. W. Schurko and S. J. Loeb, *Nat. Chem.*, 2015, **7**, 514–519.
14 V. N. Vukotic, C. A. O'Keefe, K. Zhu, K. J. Harris, C. To, R. W. Schurko and S. J. Loeb, *J. Am. Chem. Soc.*, 2015, **137**, 9643–9651.
15 R. L. Vold and G. L. Hoatson, *J. Magn. Reson.*, 2009, **198**, 57–72.
16 T. Gutmann, I. del Rosal, B. Chaudret, R. Poteau, H. H. Limbach and G. Buntkowsky, *ChemPhysChem*, 2013, **14**, 3026–3033.
17 R. H. Morris, *Coord. Chem. Rev.*, 2008, **252**, 2381–2394.
18 G. A. Facey, T. P. Fong, D. Gusev, P. M. Macdonald, R. H. Morris, M. Schlaf and W. Xu, *Can. J. Chem.*, 1999, **77**, 1899–1910.
19 F. Schröder, D. Esken, M. Cokoja, M. W. E. van den Berg, O. I. Lebedev, G. Van Tendeloo, B. Walaszek, G. Buntkowsky, H.-H. Limbach, B. Chaudret and R. A. Fischer, *J. Am. Chem. Soc.*, 2008, **130**, 6119–6130.
20 J. P. S. Mowat, S. R. Miller, J. M. Griffin, V. R. Seymour, S. E. Ashbrook, S. P. Thompson, D. Fairen-Jimenez, A.-M. Banu, T. Düren and P. A. Wright, *Inorg. Chem.*, 2011, **50**, 10844–10858.
21 J. Gonzalez, R. N. Devi, P. A. Wright, D. P. Tunstall and P. A. Cox, *J. Phys. Chem. B*, 2005, **109**, 21700–21709.
22 J. Gonzalez, R. N. Devi, D. P. Tunstall, P. A. Cox and P. A. Wright, *Microporous Mesoporous Mater.*, 2005, **84**, 97–104.
23 R. N. Devi, M. Edgar, J. Gonzalez, A. M. Z. Slawin, D. P. Tunstall, P. Grewal, P. A. Cox and P. A. Wright, *J. Phys. Chem. B*, 2004, **108**, 535–543.
24 V. J. Carter, J. P. Kujanpää, F. G. Riddell, P. A. Wright, J. F. C. Turner, C. R. A. Catlow and K. S. Knight, *Chem. Phys. Lett.*, 1999, **313**, 505–513.
25 K. Sumida, C. M. Brown, Z. R. Herm, S. Chavan, S. Bordiga and J. R. Long, *Chem. Commun.*, 2011, **47**, 1157–1159.
26 P. Canepa, N. Nijem, Y. J. Chabal and T. Thonhauser, *Phys. Rev. Lett.*, 2013, **110**, 026102(1).
27 R. F. Code and N. F. Ramsey, *Phys. Rev. A: At., Mol., Opt. Phys.*, 1971, **4**, 1945–1959.
28 B. Walaszek, A. Adamczyk, T. Pery, Y. P. Xu, T. Gutmann, N. D. Amadeu, S. Ulrich, H. Breitzke, H. M. Vieth, S. Sabo-Etienne, B. Chaudret, H. H. Limbach and G. Buntkowsky, *J. Am. Chem. Soc.*, 2008, **130**, 17502–17508.
29 V. I. Bakhmutov, *Magn. Reson. Chem.*, 2004, **42**, 66–70.
30 S. Macholl, J. Matthes, H. H. Limbach, S. Sabo-Etienne, B. Chaudret and G. Buntkowsky, *Solid State Nucl. Magn. Reson.*, 2009, **36**, 137–143.
31 F. Wehrmann, J. Albrecht, E. Gedat, G. J. Kubas, J. Eckert, H. H. Limbach and G. Buntkowsky, *J. Phys. Chem. A*, 2002, **106**, 2855–2861.
32 F. Wehrmann, T. P. Fong, R. H. Morris, H.-H. Limbach and G. Buntkowsky, *Phys. Chem. Chem. Phys.*, 1999, **1**, 4033–4041.
33 J. G. Vitillo, L. Regli, S. Chavan, G. Ricchiardi, G. Spoto, P. D. C. Dietzel, S. Bordiga and A. Zecchina, *J. Am. Chem. Soc.*, 2008, **130**, 8386–8396.
34 P. D. C. Dietzel, P. A. Georgiev, J. Eckert, R. Blom, T. Strassle and T. Unruh, *Chem. Commun.*, 2010, **46**, 4962–4964.
35 M. T. Kapelewski, S. J. Geier, M. R. Hudson, D. Stück, J. A. Mason, J. N. Nelson, D. J. Xiao, Z. Hulvey, E. Gilmour, S. A. FitzGerald, M. Head-Gordon, C. M. Brown and J. R. Long, *J. Am. Chem. Soc.*, 2014, **136**, 12119–12129.
36 L. C. Lin, J. Kim, X. Q. Kong, E. Scott, T. M. McDonald, J. R. Long, J. A. Reimer and B. Smit, *Angew. Chem., Int. Ed.*, 2013, **52**, 4410–4413.
37 W. D. Wang, B. E. G. Lucier, V. V. Terskikh, W. Wang and Y. Huang, *J. Phys. Chem. Lett.*, 2014, **5**, 3360–3365.
38 B. E. G. Lucier, H. Chan, Y. Zhang and Y. Huang, *Eur. J. Inorg. Chem.*, 2016, 2017–2024.
39 H. Lee, T. Polenova, R. H. Beer and A. E. McDermott, *J. Am. Chem. Soc.*, 1999, **121**, 6884–6894.
40 J. A. Rood, B. C. Noll and K. W. Henderson, *Inorg. Chem.*, 2006, **45**, 5521–5528.
41 T. Pham, K. A. Forrest, E. H. L. Falcao, J. Eckert and B. Space, *Phys. Chem. Chem. Phys.*, 2016, **18**, 1786–1796.
42 Y. Lu, University of Western Ontario Electronic Thesis and Dissertation Repository, 2015, Paper 3237, http://ir.lib.uwo.ca/etd/3237.

 This journal is © The Royal Society of Chemistry 2016